TECHNICAL REPORT
NATICK/TR-22/021

AD _____

BLUNT IMPACT TESTING CONSIDERATIONS

by
Tony J. Kayhart
Charles Hewitt
and
Jonathan Cyganik

April 2022

Final Report
March 2016 – August 2017

Approved for public release; distribution is unlimited.

U.S. Army Combat Capabilities Development Command Soldier Center
Natick, Massachusetts 01760-5000

DISCLAIMERS

The findings contained in this report are not to be construed as an official Department of the Army position unless so designated by other authorized documents.

Citation of trade names in this report does not constitute an official endorsement or approval of the use of such items.

DESTRUCTION NOTICE

For Classified Documents:

Follow the procedures in DoD 5200.22-M, Industrial Security Manual, Section II-19 or DoD 5200.1-R, Information Security Program Regulation, Chapter IX.

For Unclassified/Limited Distribution Documents:

Destroy by any method that prevents disclosure of contents or reconstruction of the document.

REPORT DOCUMENTATION PAGE

Form Approved
OMB No. 0704-0188

PLEASE DO NOT RETURN YOUR FORM TO THE ABOVE ADDRESS.

1. REPORT DATE *(DD-MM-YYYY)*	2. REPORT TYPE	3. DATES COVERED *(From - To)*
11-04-2022	Final	March 2016 – August 2017

4. TITLE AND SUBTITLE

BLUNT IMPACT TESTING CONSIDERATIONS

5a. CONTRACT NUMBER

5b. GRANT NUMBER

5c. PROGRAM ELEMENT NUMBER

6. AUTHOR(S)

Tony J. Kayhart, Charles Hewitt, and Jonathan Cyganik

5d. PROJECT NUMBER
16-147a

5e. TASK NUMBER

5f. WORK UNIT NUMBER

7. PERFORMING ORGANIZATION NAME(S) AND ADDRESS(ES)

U.S. Army Combat Capabilities Development Command Soldier Center
ATTN: FCDD-SCD-PMB
10 General Greene Avenue, Natick, MA 01760-5000

8. PERFORMING ORGANIZATION REPORT NUMBER

NATICK/TR-22/021

9. SPONSORING / MONITORING AGENCY NAME(S) AND ADDRESS(ES)

10. SPONSOR/MONITOR'S ACRONYM(S)

11. SPONSOR/MONITOR'S REPORT NUMBER(S)

12. DISTRIBUTION / AVAILABILITY STATEMENT

Approved for public release; distribution is unlimited.

13. SUPPLEMENTARY NOTES

14. ABSTRACT

The Army's helmet blunt impact test method is complex due to the realities of testing a helmet system. To better understand the complexities of the test method, this effort briefly investigates the roles of multiple variables: temperature dependencies of materials being evaluated, foam pad relaxation post impact, trends and repeatability of the test system. Rapid prototyping was used to create tools that could remove degrees of freedom in the test set up, potentially reducing operator dependencies.

15. SUBJECT TERMS

FOAM	HELMET PADS	BLUNT IMPACT	TEST AND EVALUATION
IMPACT	IMPACT TESTS	PADS(CUSHIONS)	IMPACT ATTENUATION
HELMETS	ELASTOMERS	HEAD(ANATOMY)	
DROP TESTS	TEMPERATURE	ARMY PERSONNEL	
TEAM WENDY	DEPENDENCIES	ACH(ADVANCED COMBAT HELMET)	

16. SECURITY CLASSIFICATION OF:			17. LIMITATION OF ABSTRACT	18. NUMBER OF PAGES	19a. NAME OF RESPONSIBLE PERSON
a. REPORT	b. ABSTRACT	c. THIS PAGE			Charles Hewitt
U	U	U	SAR	44	19b. TELEPHONE NUMBER *(include area code)* 508-206-3187

This page intentionally left blank

Table of Contents

List of Figures

List of Tables

Preface

The work reported herein was performed by the U.S. Army Natick Soldier Research, Development and Engineering Center (NSRDEC) during the period from March 2016 to September 2017 using Core Science and Technology (S&T) funds under IMTP-16-147a. The Infantry Combat Equipment Team executed the project. The objective of project 16-147a: NSRDEC Helmet Blunt Impact Testing Equipment Validation and Verification was to verify and validate that inter-laboratory drop testing equipment is equivalent across government and commercial test facilities and to identify sources of variability in current blunt impact test methodology. This report covers the latter by investigating temperature, pad relaxation, and repeatability to some extent. Further, tools are recommended to improve repeatability through removing degrees of freedom in the test set up.

Acknowledgements

The work of the following individuals and entities are acknowledged: Dr. David Colanto and Robert Dilalla for guidance and technical support; Mathew Hurley for Computer Aided Design (CAD) and additive manufacturing support; Chesapeake Testing and Aberdeen Test Center for providing their blunt impact testing services and expertise; Product Manager Soldier Protective Equipment for providing all necessary helmets for testing.

BLUNT IMPACT TESTING CONSIDERATIONS

Introduction

The work for this report was performed by the Infantry Combat Equipment Team of the Natick Soldier Research, Development and Engineering Center (NSRDEC) during the period from March 2016 to September 2017. The objective of this work was to identify sources of variability in current blunt impact test methodology and document observations made during testing.

At the completion of an inter-laboratory comparison between Army helmet blunt impact test laboratories [1] it was considered prudent to evaluate some of the potential sources of variation in the test method. This report highlights these potential sources and provides data identifying their effects on the test. The report also identifies tools which could provide improvements to the test method by eliminating human error in system set up.

Methods

The Army Test Center's (ATC) Internal Operating Procedure (IOP) for blunt impact testing [2] provides a more thorough procedure for a similar test method outlined in the Advanced Combat Helmet (ACH) purchase description CO/PD-05-04 [3]. The additional features of the ATC IOP include a standardized approach and a simplification by reducing the quantity of input variables. For example, the impact locations are precisely defined, contrary to the old method where a range is called out. An overview of the ATC IOP test method for the ACH is described next.

Preparation

Physical measurements of helmets are acquired prior to testing. They are weighed, labeled, and the helmet pads are placed into the appropriate locations as specified in the ATC IOP. Samples are evaluated under hot and cold conditions by placement in an environmental chamber at 54.4 +/-3 °C and -10 +/-3 °C respectively for at least 12 h. Ambient conditioned helmets are left at 21 +/-10 °C for at least 12 h.

A calibration procedure is also completed prior to any testing. A Modular Elastomer Pad (MEP) is centered under a hemispherical striker of radius 73 mm +/-1 mm and total mass of 5,000 g +/-100 g. The striker is simply dropped onto the MEP. The accelerations are recorded and compared to previous results to ensure the accelerometer is operating properly.

Test

Helmet impact tests are completed at seven different locations in duplicate. The second impact occurs between 60 and 120 s after the first. Each helmet is dropped onto a hemispherical anvil, apex to apex, where the lowest point of the helmet would contact the highest point of the hemispherical anvil upon impact. Striking velocity and acceleration data are recorded during each impact. The seven impact locations are conducted in the following order: Crown, Front, Rear, Left Side, Right Side, Left Nape, and Right Nape. Five of the seven impact locations can be seen in Figure 1. The front straps of the helmet are tightened to 50% or half way to maximum for all impacts and the back straps are tightened until the helmet is "snug" (left to operator's interpretation) after each impact. The helmet is positioned to what is known as Helmet Position Index (HPI), a measured distance between the brim of the helmet and the first line on the Department of Transportation (DOT) head-form. A laser gate velocity detector was used to record the velocity at every impact and a uniaxial accelerometer (vertically located at the head-form's center of gravity (CoG)) is used to record acceleration during impact.

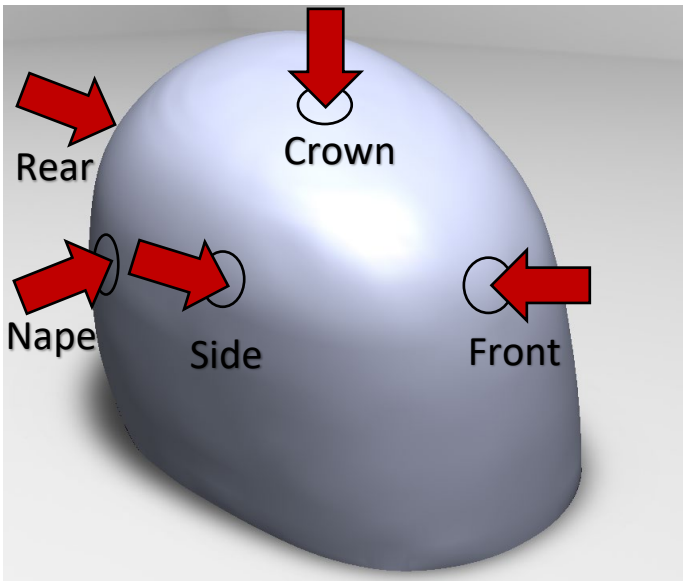

Figure 1: Impact locations shown on the DOT head-form (left nape and left side not depicted)

Temperature

In this chapter, the effects of conditioning temperature are evaluated. The ATC IOP discussed previously specifies conditioning helmets at both hot (54 °C) and cold (-10 °C) temperatures for 12 h prior to performing testing. The maximum length of exposure outside of the conditioned environment is 5 min, per the ATC IOP. A test was performed to better understand the temperature-time relationship of the helmet and pads when removed from the conditioned environment for blunt impact testing.

Temperature Drift

Method

A study was designed to simulate real time temperature changes that the helmet and helmet pad system experience during a standard drop tower experiment. An ACH was taken out of its conditioning chamber (ESPEC model BTL 433) after the required conditioning time (12 h); the cold chamber was set to -10 °C, while the hot chamber was set to 54 °C. The interior of the helmet was measured at four locations: the crown pad, the front left rectangular pad, and the two ear cups. Measurements were taken using an FLIR T650sc thermal imaging camera on a time lapse set for every 15 s, sampling for a total of 5 min. An example of the photographic data collected can be seen in Figure 2. The helmet was not disturbed after initial placement such that all measurements of a helmet are of the same point. Once completed, the helmet was returned to the conditioned ESPEC chamber for 15 min. This represents the minimum amount of time required, per the test methodology, to recondition a helmet during blunt impact testing. A repeat time lapse video was taken using the same helmet.

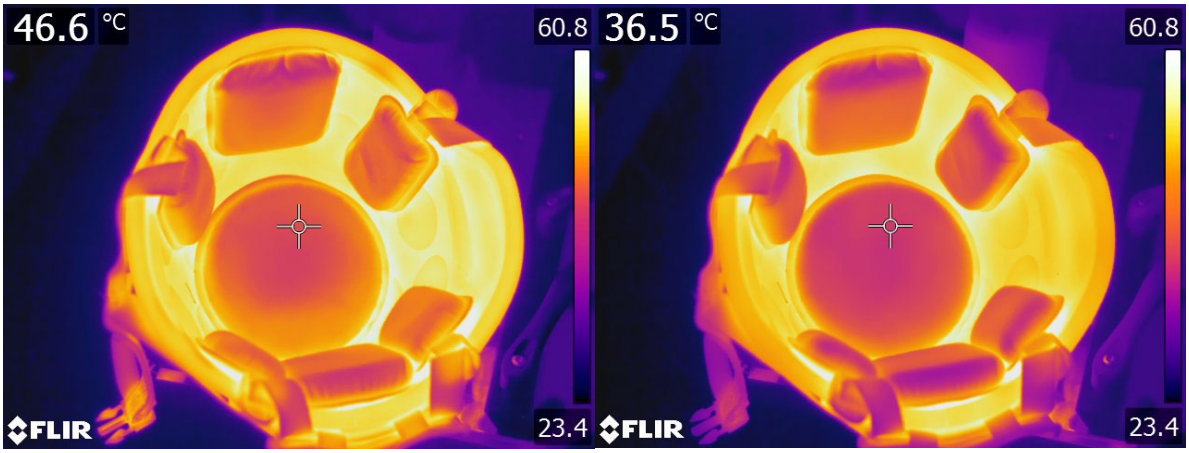

Temperature changes were compared as relative changes from starting temperature to the temperature after a given period of exposure in the room. The room was measured to be 23.5 °C the day of testing by performing a time lapse on an unconditioned helmet.

A conditioned helmet was removed from the ESPEC and placed in front of the anvil, concave up. This location was chosen because the helmet did not shift or move during the time lapse. It is important to note that since the head-form does not come in contact with the pads, there is no conductive heat loss. This investigation suggests smaller change in temperature on the interior of the helmet than would be seen during a blunt impact test.

Temperatures slowly drifted towards ambient during the 5 min time lapse recording. The results suggested that the helmet shell itself had higher thermal stability than the pads and interior of the helmet. There was difficulty measuring the same spot on each helmet, though the same spot on a given helmet was measured.

A time lapse was also performed on the exterior of the helmet, as shown in Figure 3. The helmet was removed from the chamber and mounted onto the DOT head-form. The temperature was recorded at a single point on the shell for the full 5 min time lapse series. The helmet was then returned to the ESPEC to recondition for 15 min before a second time lapse was recorded.

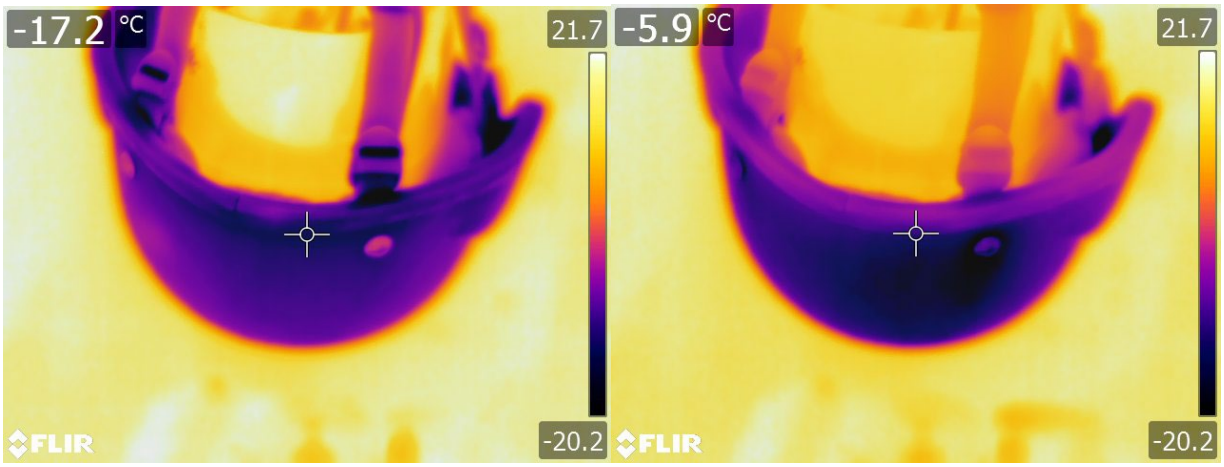

Results

The change in temperature of the helmets after being removed from the hot (54 °C) and cold (-10 °C) conditioning chambers can be seen in Figure 4 and Figure 5, respectively. Each graph depicts multiple locations through time. During the time interval of a typical impact, the ACH has drifted between 2 to 12 °C. The dotted bounding lines at 30 and 240 s represent the time frame where the two impacts (as called out in the test procedure) are most likely to occur, assuming it takes at least 30 s and up to 120 s to place the helmet onto the head-form.

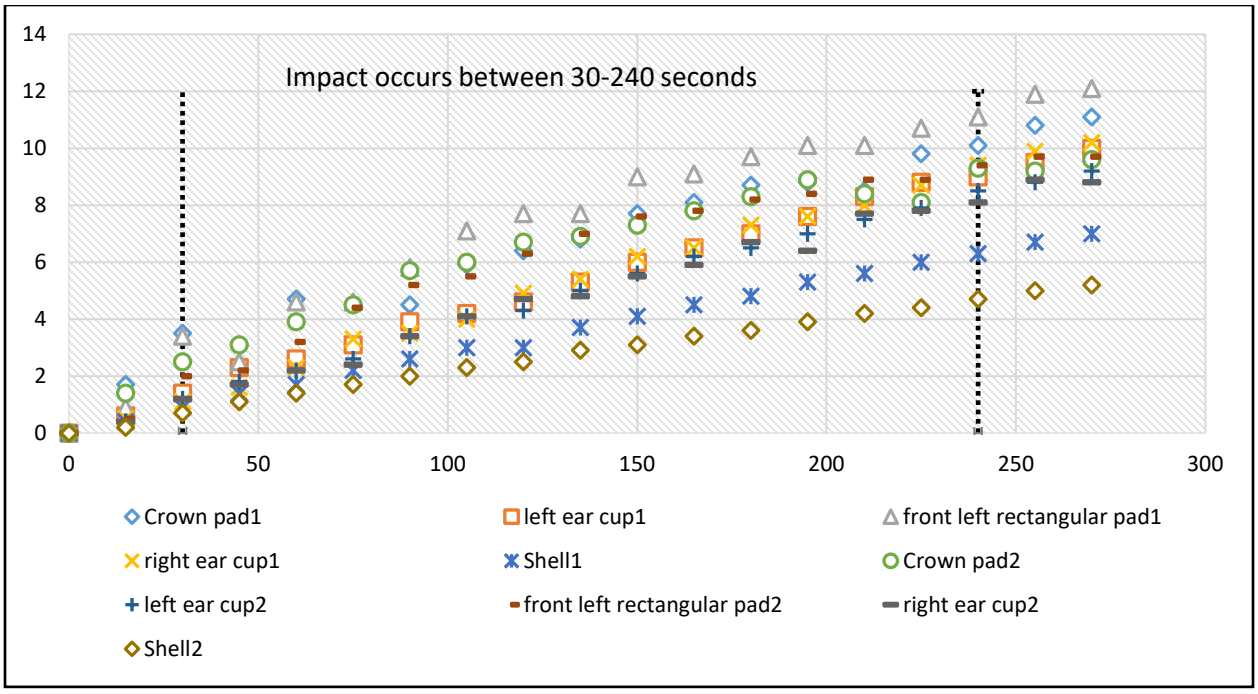

Figure 4: Temperature change over time after hot conditioning, 54 °C.

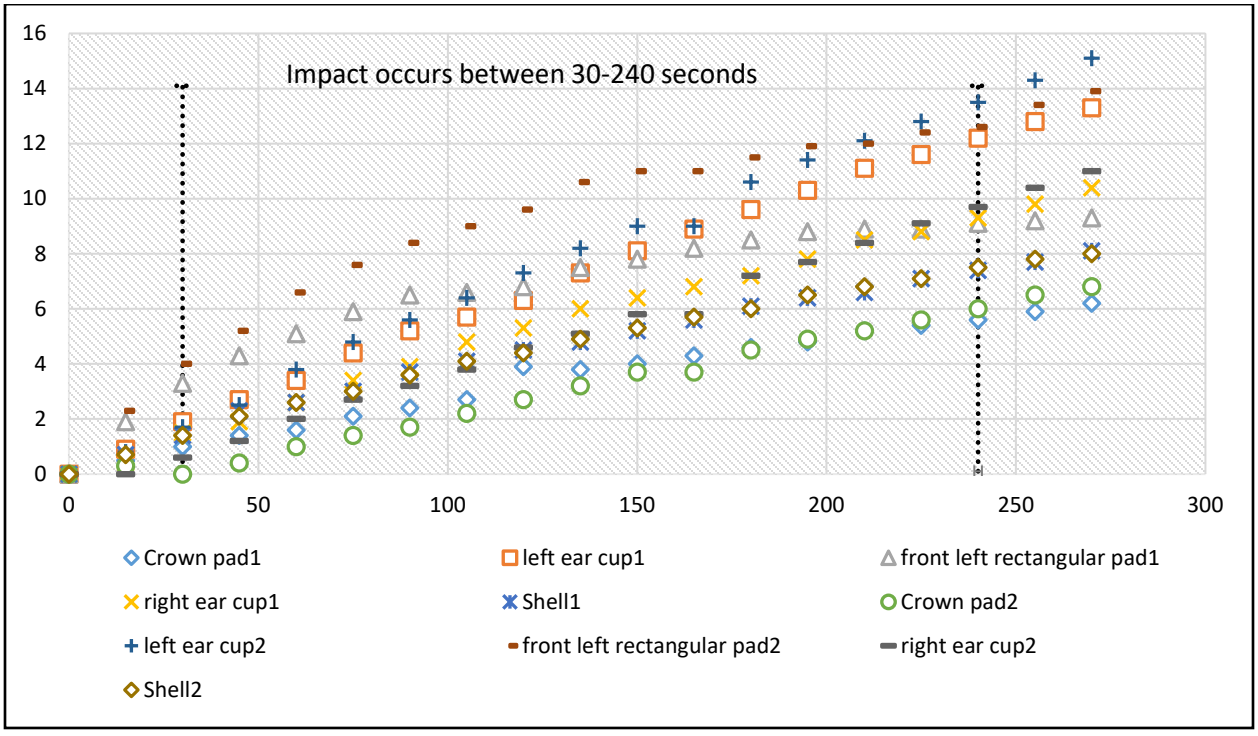

Figure 5: Temperature change over time after cold conditioning, -10 °C.

Temperature drift and peak acceleration

The results of the work described in the previous section suggested that temperature shifts of approximately 12 °C occur during helmet impact testing. In this section, the effect of that change in

temperature on the test results (peak acceleration) is evaluated by performing blunt impact tests. A limited evaluation was completed to investigate the effects of temperature shift on peak acceleration. Since the temperature of the helmet is directly correlated with the amount of time out of the environmental chamber, two impact times were chosen to represent a near ideal temperature (60 s) and an extreme temperature (240 s), where the ideal temperature is very close to the temperature of the environmental chamber and the extreme represents a change in temperature by up to 12 °C. The ideal temperature time interval of 60 s was chosen due to the difficulty of performing the impact test at exactly 30 s repeatably.

Method

Twelve ACHs with Team Wendy ZAP liner systems were conditioned at hot (54 °C) and cold (-10 °C) temperatures for 12 h. The Cadex monorail and DOT C head-form were adjusted for a crown impact location and the hemispherical anvil was positioned for apex to apex impact. Three of each condition were removed from the chamber and impacted at 60 s after removal and again 60 s after the first impact using the same method as the ATC IOP. Three of each condition were removed from the chamber and impacted at 240 s after removal and again 60 s after the first impact. Acceleration is measured at the CoG of the DOT C head-form using a uniaxial accelerometer and the peak values are recorded. Table 1 defines the test matrix.

Table 1: Temperature drift table of samples

Sample Group	Condition Temp. (°C)	Time before Impact #1 (s)	Number of specimen
Cold 1	-10	60	3
Cold 2	-10	240	3
Hot 1	54.4	60	3
Hot 2	54.4	240	3

Results

It is unlikely that the first impact will ever occur at 60 s nor 240 s; these times are considered the minimum and maximum possible during a blunt impact test. Figure 6 shows the resulting average peak acceleration in unit's gravity from three helmets at each condition and impact time. The left (diagonal lines) column for each condition is the first impact and the right (checkers) column is the second impact, which occurred 60 s after the first. The error bars are set at plus and minus one standard deviation from the mean. There is overlap between error bars between the two impact times. It appears that these data show no significant difference between the two impact times, making the 5 min out of chamber requirement valid, at least in the case of the Team Wendy ZAP liner system.

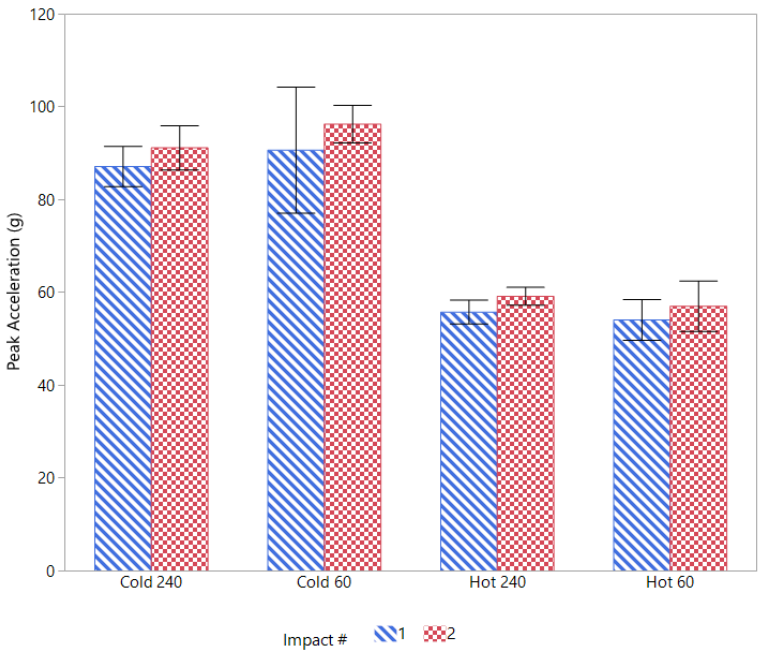

Figure 6: Temperature drift peak acceleration results

Pad Relaxation

The blunt impact test methodology calls for two sequential impacts spread by a small time difference. It is understood that a foam material will have a relaxation or recovery period prior to fully returning to its undeformed state. The test method requires the second impact to take place between 60 and 120 s after the first impact. Realistically, a second impact may occur within those first 60 s or many hours later. To better understand how much relaxation time effects the pads' ability to attenuate impact forces, a test was developed.

This test will use peak acceleration as the value to interpret pad degradation due to impacts. The first impact will occur on a pristine pad and should result in the lowest possible peak acceleration value, while any subsequent impact will result in a higher peak acceleration value. The amount of degradation can then be understood as the difference between the pristine pad value and any subsequent value.

Method

For this study, the MEP anvil is used with a hemispherical striker previously described for the calibration test. All pads were centered, by hand, on the MEP. The crown and trapezoid pads were oriented such that the pad identification information was facing the operator of the drop tower. The oblong pad was rotated 90° clockwise such that it was oriented in line with the ball arm (connecting arm between striker and carriage). The individual pads can be seen in Figure 7. Samples that required conditioning were placed in an ESPEC environmental chamber overnight at the temperature set point. Pads were tested such that they spent the least amount of time outside of an ESPEC environmental chamber and resulted in the chamber door opening as few times as possible.

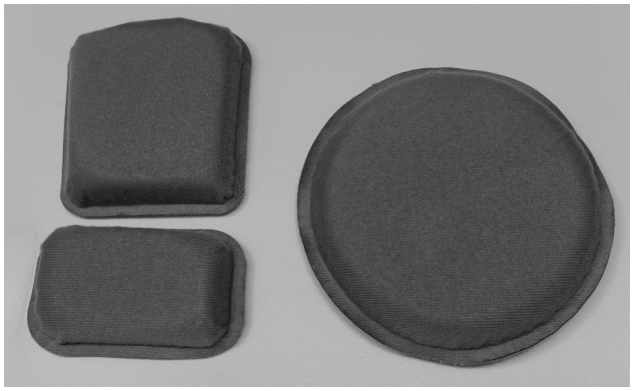

Figure 7: Trapezoidal (top left), oblong (bottom left) and crown (right)

The samples were all impacted in groups, based on their drop height. Pads were tested in the following order: 50 cm (Pad A, B and G), 97.5 cm (C, D and H), 148 cm (E, F and I). The alphabetical letters designate individual samples. The drop heights represent a doubling of impact energy at each increase. For example, the 97.5 cm impact is double the impact energy of a 50 cm impact. Each sample set was exposed to a variety of relaxation times. Where relaxation time is defined as the amount of time between the first impact and the second impact. During these time the samples will have a chance to relax or spring back to the original shape. After testing pads A-F it was determined that more testing was needed, resulting in Pads G-I. *Table 2* depicts the test matrix.

Table 2: Pad Relaxation Test Matrix

Sample Shape	Drop Height (cm)	Relaxation Time (min)	Temperature
Oblong	50	0.5, 1, 2, 5, 30, 120, 1440	Cold, Ambient, Hot
Square	50	0.5, 1, 2, 5, 30, 120, 1440	Cold, Ambient, Hot
Round	50	0.5, 1, 2, 5, 30, 120, 1440	Cold, Ambient, Hot
Oblong	97.5	0.5, 1, 2, 5, 30, 120, 1440	Cold, Ambient, Hot
Square	97.5	0.5, 1, 2, 5, 30, 120, 1440	Cold, Ambient, Hot
Round	97.5	0.5, 1, 2, 5, 30, 120, 1440	Cold, Ambient, Hot
Oblong	148	0.5, 1, 2, 5, 30, 120, 1440	Cold, Ambient, Hot
Square	148	0.5, 1, 2, 5, 30, 120, 1440	Cold, Ambient, Hot
Round	148	0.5, 1, 2, 5, 30, 120, 1440	Cold, Ambient, Hot

The 30 min, 2 h and 24 h samples were returned to the environmental chamber for conditioning after the first round of impacts. The other samples remained outside the environmental chamber between impacts. The 5 min, 30 min, 2 h and 24 h samples were each impacted once. The 5 min samples were then impacted again. The other samples were each returned to the environmental chamber for the remainder of their relaxation time. The 60 s and 120 s relaxation samples were impacted in pairs, such that each drop height was completed before moving to the next height. The 30 s samples were impacted such that a pad was impacted twice before moving on to the next pad.

Results

In each of the following graphs, the average peak acceleration (g) is depicted on the y axis and the time between first and second impact is depicted on the x axis. Time 0 represents first impact while all other relaxation times represent the second impact, which occurs at the denoted time. The dotted lines are for visual purposes to help differentiate test conditions and not meant to be used for any analytical purposes.

It can be seen in Figures 8, 9, and 10 that the pads do not fully recover even after 24 h. The pad type had a significant effect on average peak acceleration, likely due to the amount of contact area during impact. This is especially noticeable with the oblong pads. Cold increases stiffness which is beneficial to the pads with a smaller impact surface area (oblong) while the Hot condition decreases stiffness which may be beneficial for a larger surface area (trapezoidal or crown). Tabulated results can be found in Appendix A.

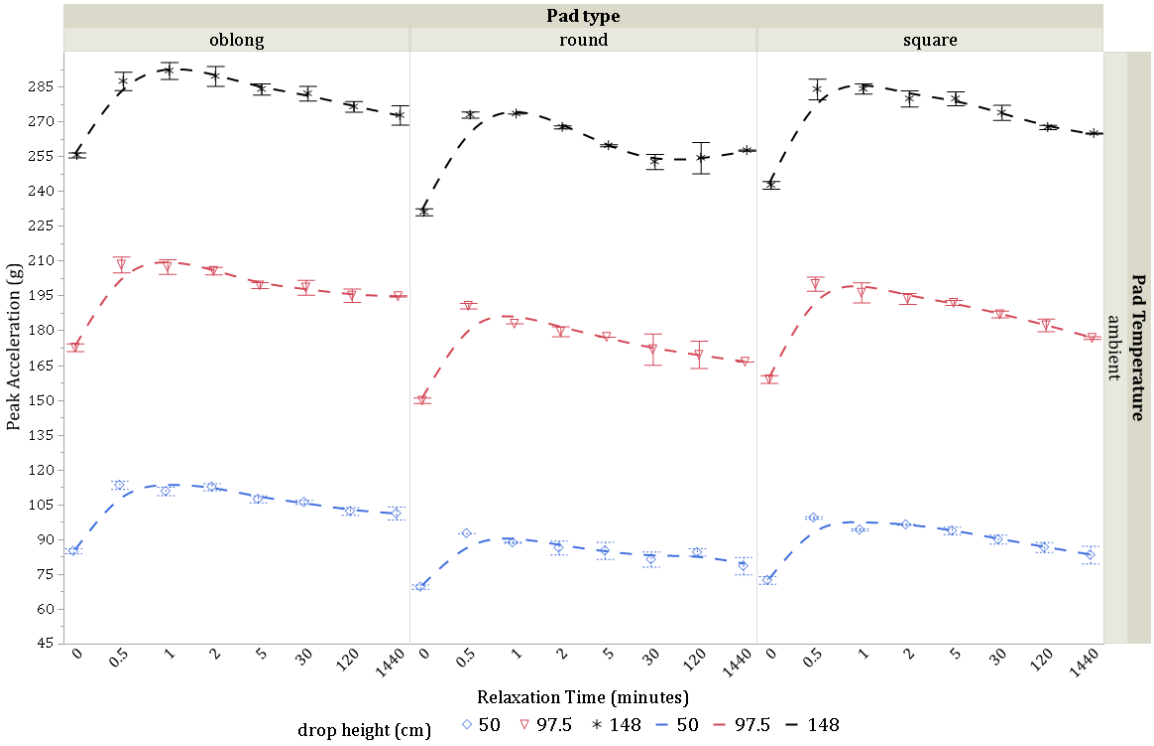

Figure 8: Pad relaxation – ambient condition. Error bars represent 1 standard deviation from the mean

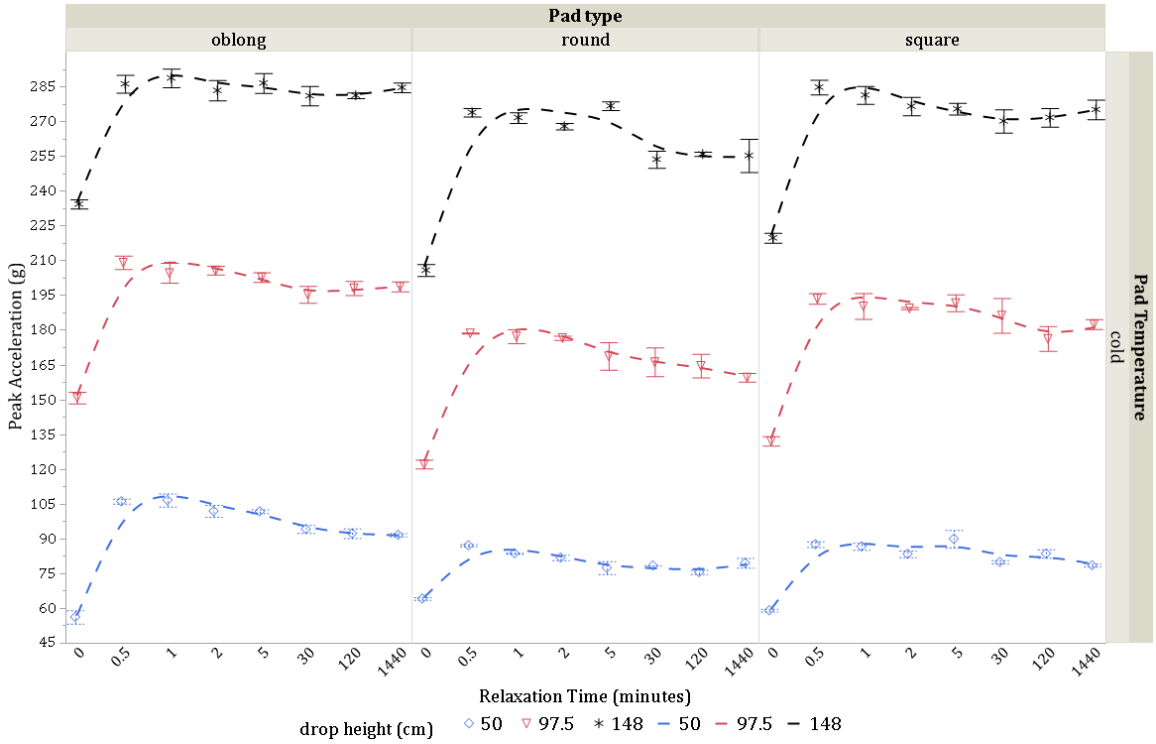

Figure 9: Pad Relaxation – Cold condition

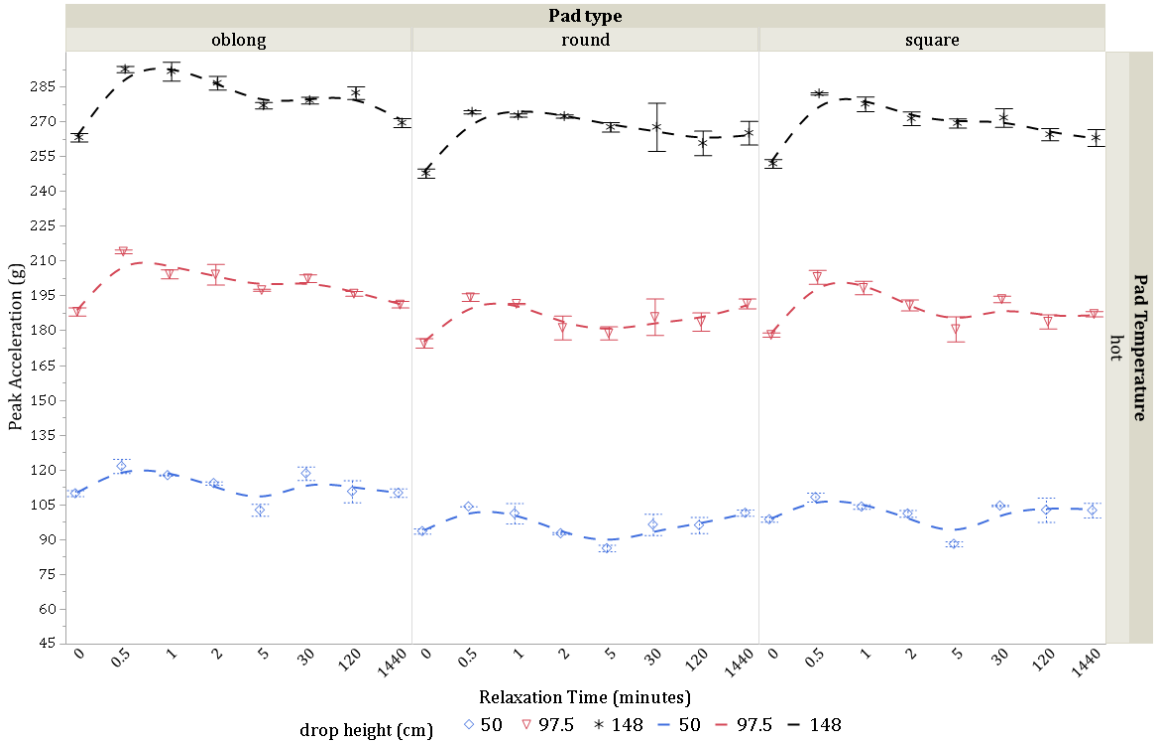

Figure 10: Pad Relaxation – Hot Condition

Sensors

In this section, the repeatability of NSRDEC's test rig sensors are evaluated. It is important that velocity and acceleration data are highly repeatable to ensure consistency between experiments.

Accelerometer and Velocimeter Variability

Method

The purpose of this document is to assess variability and repeatability of accelerometer sensors used with the Cadex drop tower. Data from three accelerometers were compared across four different drop heights of the Cadex drop tower. Three accelerometers were purchased of the same brand (PCB) and model (353B18). To compare the accelerometers, multiple (N= 21) impacts were performed in repetition on the MEP using the hemispherical striker at four heights. All accelerometers were calibrated prior to testing. The accelerometer sensors' serial numbers were 185404, 201248, and 201249. The heights of drop were chosen as 25 cm, 50 cm, 97.5 cm, and 148 cm. Striking velocity data were recorded during each test as well, using the velocimeter provided with the Cadex drop tower. The Velocimeter is the combination of a laser gate and flag affixed to the carriage (or bearing slide the striker is attached). Velocity is calculated by recording the time duration that the laser is blocked by the flag, where the flag has a known length. Each sensor was dropped a total of 21 times from each height listed. All impacts were performed using the hemispherical striker previously described and MEP anvil.

Results

The average maximum acceleration values for each of the sensors at each drop height are displayed in Figure 11. Very little appreciable difference exists between sensors at a given height of drop. Additionally, each sensor at each drop height exhibits a coefficient of variation much less than one, indicating there is minimal spread in the data. With the exception of the SN201249 dropped from 148 cm the spread between sensors was minimal as well. This chart indicates good linearity in sensor response for all three accelerometers. The entire data set can be found in Appendix B.

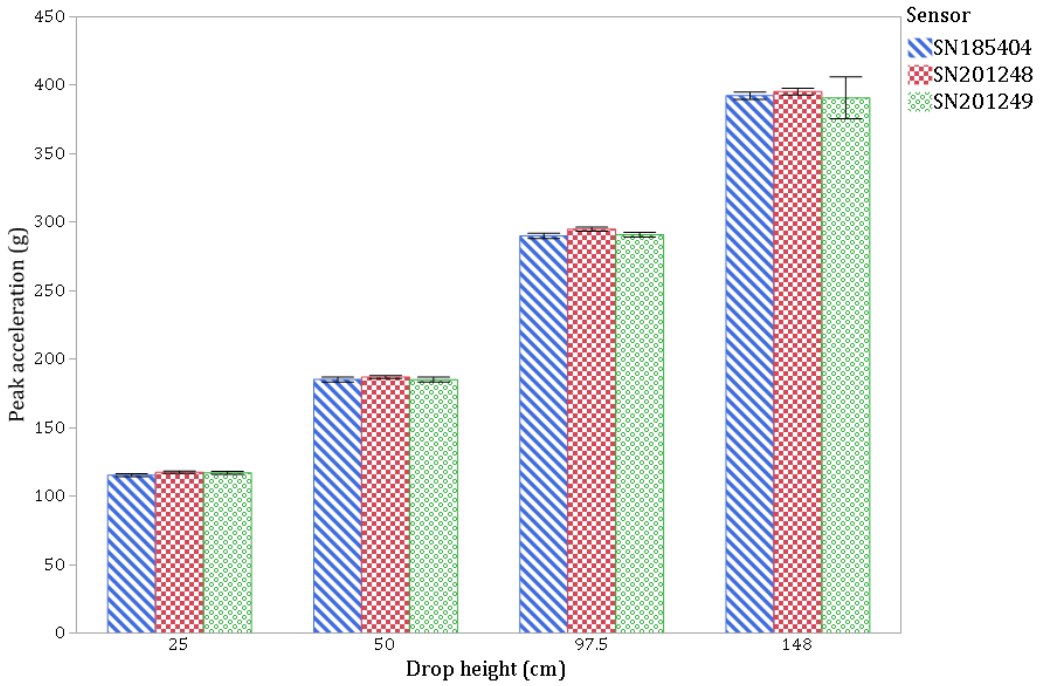

Figure 11: Peak acceleration at multiple heights

The velocity results are shown in Table 2.

Table 3: Drop height variation statistics

Statistic	**25 cm**	**50 cm**	**97.5 cm**	**148 cm**
Mean Velocity (m/s)	2.148	3.076	4.306	5.311
Std Dev	0.012	0.014	0.023	0.028
N	51	50*	51	51
Mean Acceleration (g)	116.663	185.837	292.073	392.986
Std Dev	1.348	1.776	2.703	9.061
N	51	51	51	51

*velocity was not recorded for one impact at 50 cm drop height.

Due to the qualitative closeness of acceleration data between sensors, narrowness of variance, and linearity of sensors, it was not thought necessary to perform statistical analysis on the data. The figures presented in this document strongly indicate that the accelerometer sensors used in the setup contribute negligible variance to the data collected. Variability in the recorded measurements of blunt impact testing of armor and equipment is nearly entirely caused by other sources. A similar analysis of system mass can be found in Appendix C.

Trends

Using data collected for a separate study [1]; the overall trends in ACH blunt impact testing are analyzed. These data represent the results from the ATC IOP [2] evaluating the ACH from three test laboratories. These data include all three environmental conditions (hot, cold, ambient), all seven impact locations: two impacts per location and two helmets for every condition per test laboratory. All the data are aggregated assuming that test laboratory differences (if any) do not affect the general trends. These data are also compared to historical data in Appendix D.

Helmet Size

Aggregating all impact locations, conditions and impacts together, the data can be broken out by helmet size. The larger helmets tend to result in a reduced peak acceleration and curiously a reduction in standard deviation as seen in Figure 12. The number at the center of each column represents the peak acceleration of the head-form in gravities (g) and the error bar represents plus and minus one standard deviation from the mean. All figures in this section are depicted in the same manner.

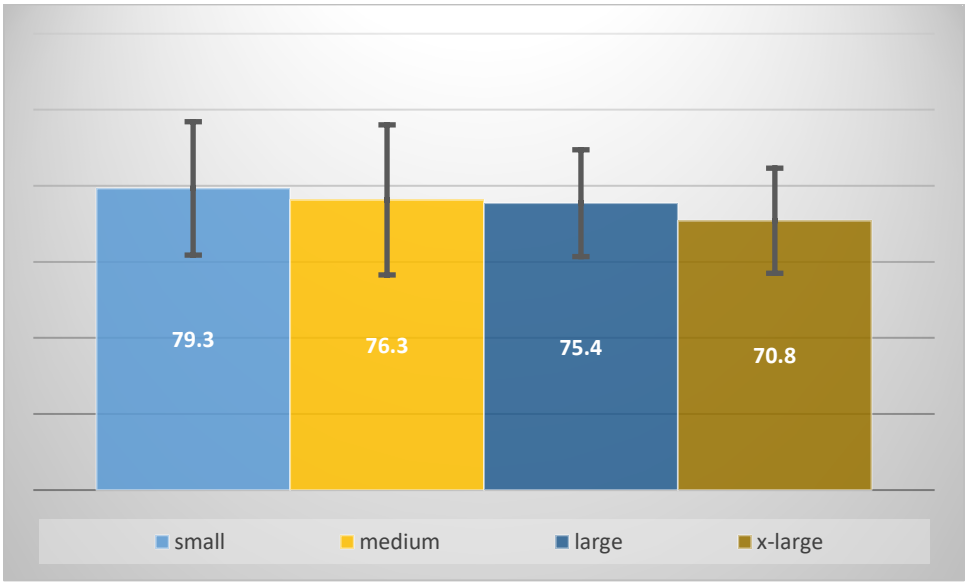

Figure 12: Break Out by Size

Breaking out environmental conditioning, the data show that the cold and ambient conditions are driving the trend of decreasing peak acceleration with increasing helmet size (Figure 13). This is likely due to increased pad stiffness being favorable for larger and hence heavier helmets. This is thought to be due to the reduced pad interaction at each impact location as the pads are more spread apart, whereas the smaller helmets have increased pad interaction due to the pads being spaced closer together, making increased individual pad stiffness a net negative.

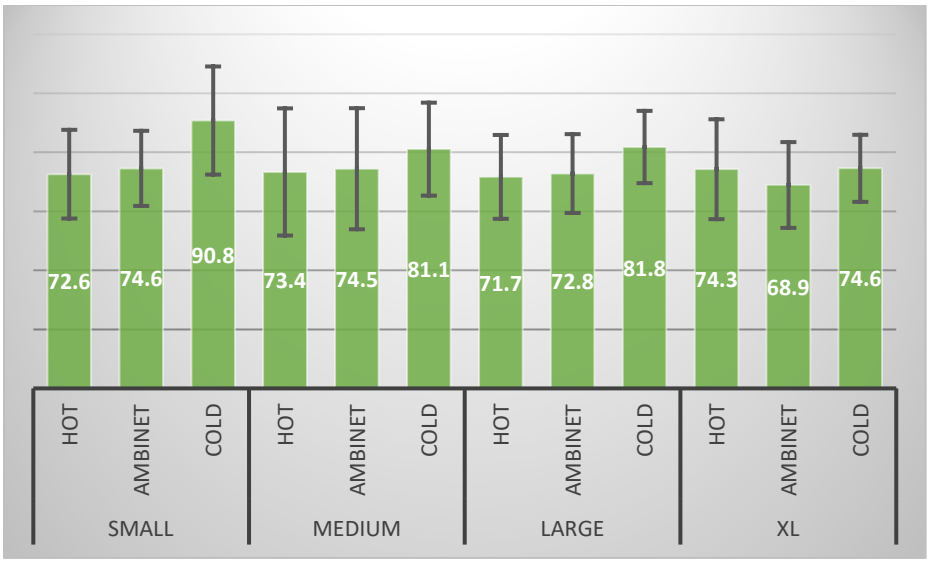

Figure 13: Break Out by Size – by Condition

Impact Location

In Figure 14 the data are aggregated by impact location for all helmet sizes and temperature conditions. This leaves only the variable of impact location to compare. In Figure 14 a direct comparison of the impact locations can be seen. Notably the front impact locations shows the highest peak acceleration as well as the highest standard deviation. This is thought to be caused by the difference in curvature between the ACH and the DOT head-form in the front region.

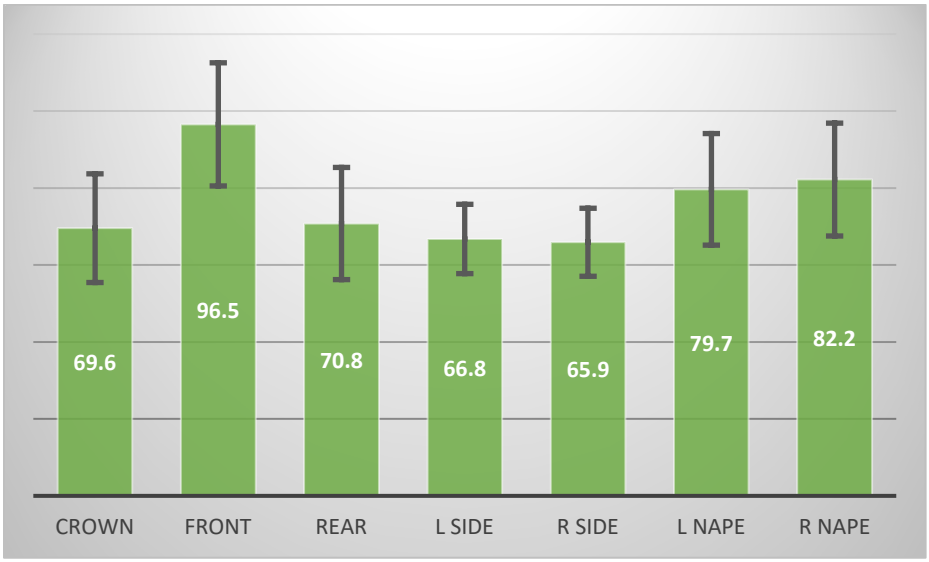

Figure 14: Break out by Impact Location (All Laboratories, Sizes and Conditions)

Impact Number

As expected, the second impact results in a higher peak acceleration as depicted in Figure 15. The increased peak acceleration is dependent on the helmet liner's ability to spring back between impacts. As discussed previously in the pad relaxation section, the Team Wendy pads do not have enough time to fully relax between the first and second impact, reducing their ability to attenuate energy.

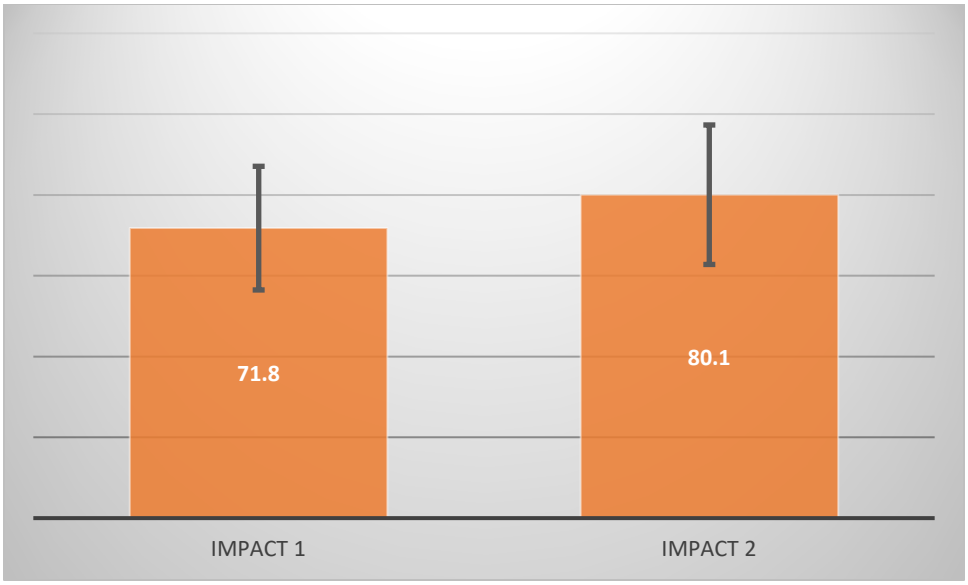

Figure 15: Aggregate by Impact Number

Similarly, Figure 16 shows the first and second impacts broken out by temperature. Each temperature condition shows a similar degradation in impact attenuation between the first and second impact due to lack of recovery time between impacts. This is represented by the increased acceleration experienced by the head-form. If the pads had not undergone some type of change the acceleration would remain the same between impacts.

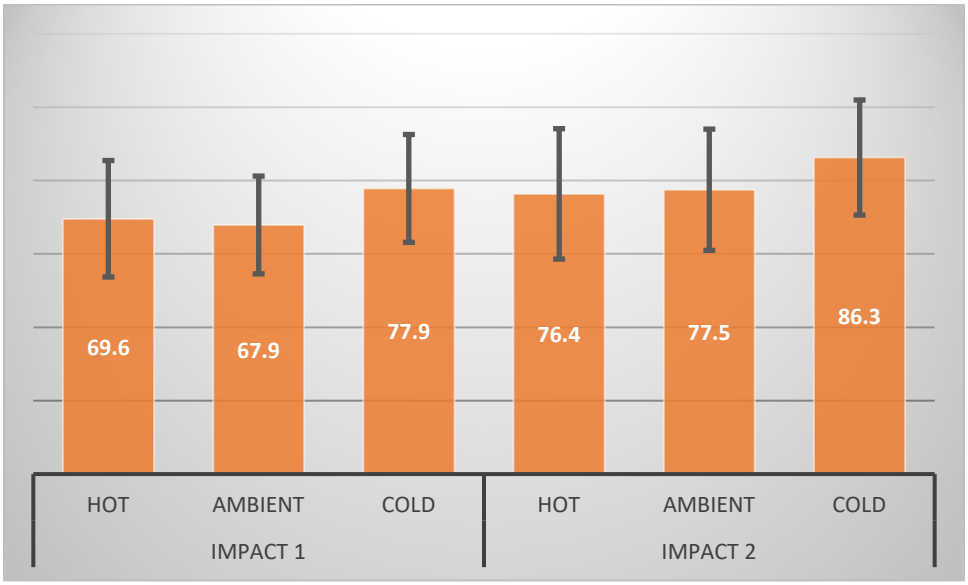

Figure 16: Aggregate by Impact Number – By Condition

Environmental Condition

On average the cold condition displays the highest peak acceleration as depicted in Figure 17. It is thought that this is due to the increased material stiffness at the cold temperature, which appears to have a negative effect on most helmet sizes.

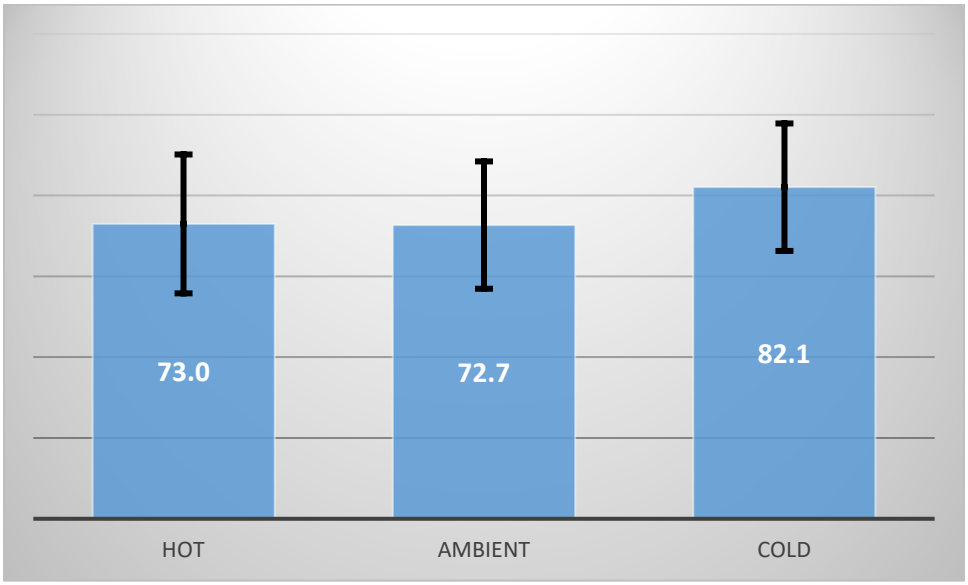

Figure 17: Break Out by Condition

When comparing the peak accelerations by condition and impact location, the data show the cold condition with the highest peak acceleration in all impact locations except for the front impact location (Figure 18). Again this appears to be due to the difference in curvature at the front impact location. The front impact location is thought to have minimal to no interaction with the crown pad and no interaction with the rear pads. Thus the front impact location benefits from increased pad stiffness.

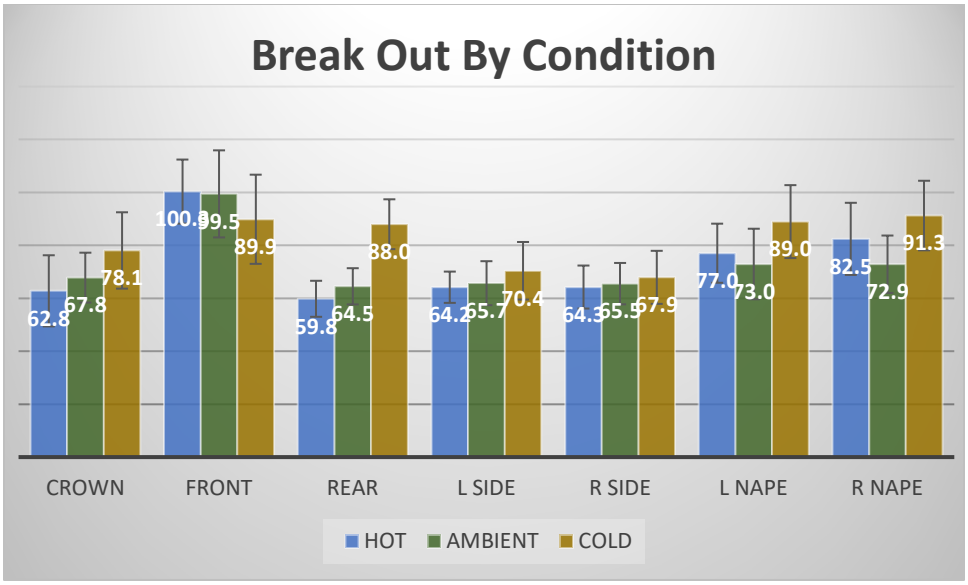

Figure 18: Break Out by Condition – by Impact Location

Alignment Tooling

Head-form Alignment Tool (HAT)

Difficulty in aligning the head-form to each of the seven locations is due to three axes of freedom on the ball arm. Measuring all three axes of rotation at each impact location while ensuring the position of the head-form is the same for each test is problematic. Further complicating the issue, when tightening the four bolts that clamp the head-form into position, the assembly often moves on one of those three axes. A method to remedy this problem was devised. The Head-form Alignment Tool (HAT) was developed, depicted in Figure 19. This rapid prototyped tool is placed over the head-form and the anvil. The tool enables rapid location of each of the seven impact locations and accounts for all three axes of freedom.

Figure 19: Suite of HATs

To use the HAT, a DOT head-form is attached to the Cadex carriage assembly, leaving the four collar bolts loose enough to spin the head-form on the ball arm. As seen in Figure 20, the corresponding HAT-half slides over the DOT head-form. The Cadex base plate is positioned a distance from the edge of the platform, which lines up with the CoG of the DOT head-form or the vertical center of the ball-portion of the arm. Next, the HAT locator base is fitted onto the base plate. From here the head-form and carriage assembly is lowered onto the HAT locator base (tool with hand grip). Once the HAT's alignment pin to fit in the alignment base receptor the head-form bolts can be tightened and the HAT removed. The head-form is now located in the correct position in all three rotational axes and ready for use. This new system theoretically reduces test to test error by standardizing the way in which the head-form is positioned.

Figure 20: Crown position using the HAT

Pad Locator

The location of the individual pads inside the helmet is specified by the ATC IOP. However, it can be difficult to repeatedly place the pads in the exact same place every time. A rapid prototyped Bending Alignment Tool (BAT) depicted in Figure 21, was developed using a flexible material so that the device can easily be placed into a size large ACH. Pads can be placed in their designated locations and the BAT can be easily removed due to its flexibility (Figure 22).

This new tool may reduce the helmet to helmet variability in pad placement, further standardizing the test method.

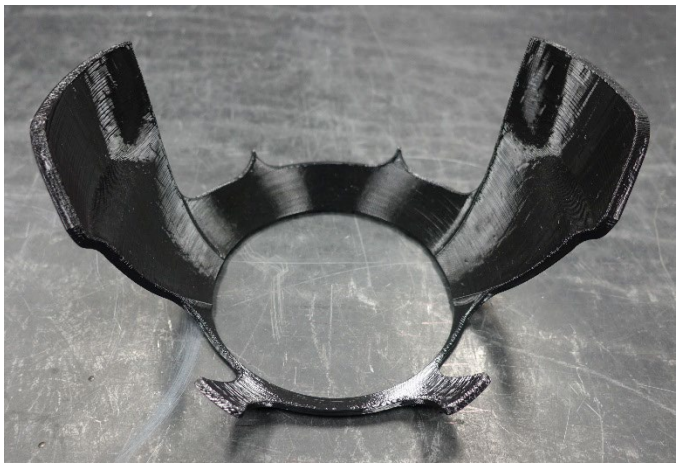

Figure 21: BAT

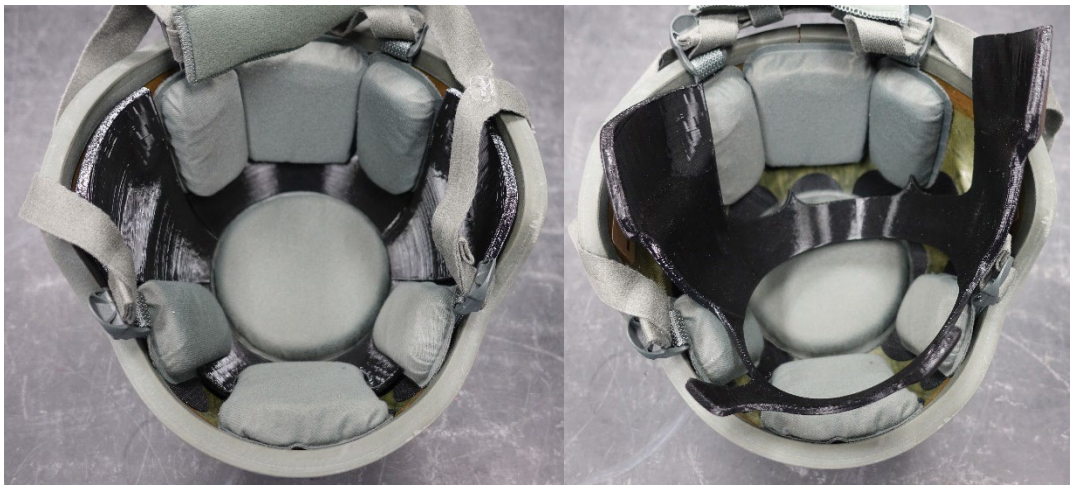

Figure 22: BAT with pads (left) BAT removed (right)

Conclusion

Test methodology variables, trends and methods to mitigate variability were discussed. The error in sensors and the data acquisition systems currently in use by the Army for this type of testing appears to be adequate, or at least the sensor error is well within the noise of the test methodology. Trends were evaluated showing substantial difference between helmet sizes, impact locations and temperature effects. It is thought that the fit between the DOT head-forms and the ACH is not perfect, causing the majority of these large swings in acceleration between the variables. This could be argued to be a good thing, providing data at the extreme.

A pad relaxation test was described and implemented, providing a way to analyze the time required for a pad system to spring back after impact. This test also showed how the time between the first and second impact can greatly affect the test results. Thus a test performed with more consistent timing between impacts should prove more repeatable.

The temperature loss during the time in which helmets are removed from the environmental chamber was evaluated in a simple manner. It was found that the maximum of 5 min out of chamber time appears to be reasonable for the current ACH but new helmet systems with lower heat capacitance may be more affected by this variable. To truly remove this variable, the test would need to be completed in an environmental chamber, making the test equipment prohibitively expensive.

Other variables such as impact location, pad placement, and anvil alignment were not evaluated. These variables are likely to cause variation in the test but are difficult to evaluate due to having an unlimited number of possibilities. The alignment tools described or similar equipment could be used to help eliminate these variables, especially in the case of someone new to the test method, potentially reducing the “learning curve” error.

This document reports research undertaken at the U.S. Army Combat Capabilities Development Command Soldier Center, Natick, MA, and has been assigned No. Natick/TR-22/021 in a series of reports approved for publication

References

[1] C. H. J. C. Tony Kayhart, "Inter-laboratory Combat Helmet Blunt Impact Test Method Verification and Validation," Natick Soldier RD&E Center, Natick, MA, 2017.

[2] M. Bruggeman, "INTERNAL OPERATING PROCEDURE No. 029 REV E - BLUNT IMPACT TESTING PROCEDURE FOR COMBAT HELMETS," ABERDEEN TEST CENTER WARFIGHTER DIRECTORATE MATERIALS & MEASUREMENTS TEST BRANCH.

[3] P. S. E. TMD, ""“Purchase Description, Helmet, Advanced Combat (ACH)” CO/PD-05-04 pp. 32," Program Executive Office – Soldier, Fort Belvoir, VA, 2007.

Appendix A – Pad Relaxation Data Table

			peak acceleration (g)																			
			relaxation time (minutes)																			
			0			0.5			1			2			5			30			120			1440		
Pad type	drop height (cm)	Pad temperature	Mean	Std Dev	N	Mean	Std Dev	N	Mean	Std Dev	N	Mean	Std Dev	N	Mean	Std Dev	N	Mean	Std Dev	N	Mean	Std Dev	N	Mean	Std Dev	N
oblong	148	ambient	255.6	4.832	21	287.4	6.835	3	291.9	6.311	3	289.6	7.4	3	284	4.13	3	282.1	5.415	3	276.5	3.968	3	272.8	7.26	3
		cold	234.3	8.991	21	286.1	6.637	3	288.7	6.995	3	283.3	7.563	3	286.5	7.398	3	281	7.251	3	281.2	2.139	3	284.6	3.579	3
		hot	263.2	8.468	22	292.5	2.329	3	291.6	7.017	3	286.6	5.138	3	276.9	2.35	3	279.1	2.554	3	282.4	4.738	3	269.5	3.293	3
	50	ambient	85.06	5.036	21	113.5	3.121	3	110.8	3.208	3	112.7	2.65	3	107.4	2.536	3	106.1	1.563	3	102.2	2.948	3	101.3	4.882	3
		cold	56.2	13.21	21	106.1	1.852	3	106.6	4.854	3	101.9	4.45	3	101.8	1.405	3	94.13	2.901	3	92.27	3.585	3	91.63	1.155	3
		hot	109.9	5.799	21	121.6	5.235	3	117.7	0.404	3	114.2	1.222	3	102.7	4.493	3	118.5	5.029	3	110.7	8.182	3	110.1	3.166	3
	97.5	ambient	172.7	7.477	21	208.4	5.927	3	207.5	5.519	3	205.7	2.811	3	199.5	2.261	3	198.6	5.519	3	195.1	4.954	3	194.8	0.493	3
		cold	150.8	11.53	21	209.1	5.014	3	204.6	7.466	3	205.7	3.25	3	202.8	3.564	3	195.3	6.269	3	198.1	5.274	3	198.7	3.667	3
		hot	188.1	7.945	20	214	1.473	3	204.3	3.398	3	204.2	7.702	3	197.5	0.764	3	202.5	2.836	3	195.9	1.8	3	191.2	2.419	3
round	148	ambient	231.1	5.689	14	273	1.909	2	273.4	0	2	267.7	0.919	2	259.8	0.636	2	252.8	4.596	2	254.4	9.546	2	257.7	0.354	2
		cold	205.8	9.759	14	273.9	2.616	2	271.6	3.253	2	267.9	1.98	2	276.7	2.616	2	253.6	5.233	2	255.9	1.273	2	255.3	10.11	2
		hot	247.7	7.501	14	274.1	0.99	2	272.7	0.99	2	272.3	0.99	2	267.7	2.899	2	267.7	14.64	2	260.7	7.495	2	265.1	7.212	2
	50	ambient	69.64	3.428	14	92.7	0	2	88.75	0.354	2	86.45	4.172	2	85.2	5.233	2	81.45	4.596	2	84.5	2.263	2	78.65	5.303	2
		cold	64.14	2.086	14	87.15	0.636	2	83.7	0.283	2	81.85	1.626	2	77.45	3.889	2	78.4	0	2	75.6	1.273	2	79.55	2.899	2
		hot	93.56	4.338	14	104.2	0	2	101.2	6.223	2	92.65	0.636	2	86.2	1.98	2	96.4	6.505	2	96.15	4.879	2	101.5	1.909	2
	97.5	ambient	149.9	4.447	14	190.7	1.626	2	183	0	2	179.6	2.97	2	177.3	0	2	172	9.546	2	169.7	8.273	2	166.6	0	2
		cold	122.1	7.071	14	178.7	0.354	2	177.3	4.243	2	176.6	1.273	2	168.8	8.415	2	166.2	8.768	2	164.6	7.212	2	159.6	2.616	2
		hot	174.6	7.629	14	194.4	2.333	2	191.6	0.354	2	181.2	7.212	2	178.9	3.96	2	185.9	11.1	2	183.8	5.586	2	191.6	2.97	2
square	148	ambient	242.7	7.504	21	284	7.711	3	284.1	3.79	3	279.9	6.032	3	279.9	5.217	3	273.9	5.63	3	267.6	1.637	3	265	0.289	3
		cold	219.7	9.623	21	284.7	5.501	3	281.3	6.59	3	276.5	6.846	3	275.4	4.325	3	270.1	8.682	3	271.7	6.957	3	275.1	7.275	3
		hot	251.9	8.627	21	282.1	0.808	3	277.6	5.45	3	271.3	5.006	3	269.3	3.439	3	271.6	6.917	3	264.5	4.594	3	263.1	6.298	3
	50	ambient	72.49	7.415	21	99.43	0.924	3	94.27	0.737	3	96.47	0.351	3	93.8	2.805	3	90.07	3.355	3	86.67	3.667	3	83.4	6.56	3
		cold	59.09	2.769	21	87.6	2.163	3	86.67	2.641	3	83.4	2.587	3	89.93	6.649	3	79.97	1.206	3	83.57	3.156	3	78.53	1.069	3
		hot	98.67	5.213	21	108.2	3.361	3	104.1	1.677	3	101.1	2.485	3	88.07	1.901	3	104.6	0.513	3	102.7	9.067	3	102.5	5.485	3
	97.5	ambient	159	7.636	21	200.1	5.258	3	196.4	7.494	3	193.7	4.005	3	192	1.848	3	187	2.479	3	182.4	4.734	3	176.9	1.021	3
		cold	132.1	9.234	21	193.6	3.98	3	190.3	9.638	3	189.4	0.814	3	191.7	6.296	3	186.3	13.01	3	176.3	9.278	3	182.5	3.7	3
		hot	178.2	4.153	21	203.1	5.163	3	198.4	5.014	3	190.9	4.104	3	180.6	9.4	3	193.5	2.454	3	183.9	5.311	3	187.2	1.986	3

This page intentionally left blank

Appendix B – Accelerometer and Velocimeter Repeatability Data

Sensor	Impact number	Peak acceleration (g)	Velocity (m/s)	Drop height (cm)
SN185404	1	394.3	5.3548	148
SN185404	2	388.2	5.2627	148
SN185404	3	393.3	5.3138	148
SN185404	4	395.2	5.3447	148
SN185404	5	395.7	5.3287	148
SN185404	6	392.9	5.3242	148
SN185404	7	394.3	5.3432	148
SN185404	8	392.9	5.3117	148
SN185404	9	395.2	5.3452	148
SN185404	10	393.8	5.3456	148
SN185404	11	393.8	5.3379	148
SN185404	12	387.7	5.2817	148
SN185404	13	387.3	5.2718	148
SN185404	14	390.5	5.313	148
SN185404	15	393.8	5.2994	148
SN185404	16	393.3	5.3306	148
SN185404	17	390.5	5.2897	148
SN185404	1	114.5	2.1506	25
SN185404	2	114	2.1264	25
SN185404	3	115	2.1363	25
SN185404	4	115.4	2.1402	25
SN185404	5	116.4	2.1235	25
SN185404	6	113.6	2.1382	25
SN185404	7	115.4	2.1264	25
SN185404	8	117.8	2.1479	25
SN185404	9	115.4	2.1399	25
SN185404	10	116.4	2.1479	25
SN185404	11	115	2.1462	25
SN185404	12	115	2.1417	25
SN185404	13	115.4	2.1322	25
SN185404	14	116.8	2.1249	25
SN185404	15	115.9	2.1375	25
SN185404	16	113.6	2.1262	25
SN185404	17	116.4	2.1361	25
SN185404	1	183.4	3.0853	50
SN185404	2	182.9	3.0734	50
SN185404	3	183.9	3.063	50

SN185404	4	182.5	3.0812	50
SN185404	5	183.9	3.0817	50
SN185404	6	186.2	3.0865	50
SN185404	7	184.3	3.0865	50
SN185404	8	184.8	3.099	50
SN185404	9	188.1	3.1066	50
SN185404	10	187.1	3.0998	50
SN185404	11	183.4	3.0767	50
SN185404	12	186.7	3.1008	50
SN185404	13	188.1	3.0849	50
SN185404	14	185.3	3.0962	50
SN185404	15	186.2	3.0915	50
SN185404	16	186.2	3.0881	50
SN185404	17	186.2	3.0788	50
SN185404	1	288.6	4.2912	97.5
SN185404	2	292.8	4.329	97.5
SN185404	3	289.5	4.2829	97.5
SN185404	4	288.6	4.2839	97.5
SN185404	5	291.9	4.3306	97.5
SN185404	6	291.4	4.2936	97.5
SN185404	7	290.5	4.3211	97.5
SN185404	8	290	4.2831	97.5
SN185404	9	289.1	4.2958	97.5
SN185404	10	292.3	4.3456	97.5
SN185404	11	293.2	4.3591	97.5
SN185404	12	290.9	4.2939	97.5
SN185404	13	290.9	4.3433	97.5
SN185404	14	285.3	4.2683	97.5
SN185404	15	289.5	4.292	97.5
SN185404	16	289.1	4.2761	97.5
SN185404	17	289.5	4.314	97.5
SN201248	1	395.1	5.3161	148
SN201248	2	399.3	5.343	148
SN201248	3	397	5.3268	148
SN201248	4	398.8	5.3232	148
SN201248	5	398.4	5.3168	148
SN201248	6	397.4	5.331	148
SN201248	7	397.4	5.3389	148
SN201248	8	395.6	5.3054	148
SN201248	9	391.9	5.2843	148
SN201248	10	396.5	5.316	148

SN201248	11	392.8	5.3234	148
SN201248	12	395.6	5.3286	148
SN201248	13	393.3	5.2954	148
SN201248	14	391.9	5.2909	148
SN201248	15	391.9	5.3164	148
SN201248	16	397	5.3413	148
SN201248	17	393.8	5.3289	148
SN201248	1	117.6	2.1421	25
SN201248	2	117.1	2.1602	25
SN201248	3	118	2.1731	25
SN201248	4	116.7	2.1461	25
SN201248	5	118	2.1449	25
SN201248	6	118	2.1506	25
SN201248	7	118.5	2.1593	25
SN201248	8	115.7	2.1417	25
SN201248	9	116.7	2.1429	25
SN201248	10	116.2	2.1523	25
SN201248	11	118.5	2.1562	25
SN201248	12	118.5	2.1483	25
SN201248	13	117.1	2.1547	25
SN201248	14	116.7	2.1496	25
SN201248	15	118.5	2.1661	25
SN201248	16	117.1	2.1619	25
SN201248	17	118.5	2.144	25
SN201248	1	187.2	3.0822	50
SN201248	2	188.1	0.2682	50
SN201248	3	186.7	3.081	50
SN201248	4	184.9	3.0439	50
SN201248	5	187.2	3.0796	50
SN201248	6	187.7	3.0804	50
SN201248	7	186.3	3.0692	50
SN201248	8	186.7	3.0547	50
SN201248	9	188.1	3.0758	50
SN201248	10	189	3.0809	50
SN201248	11	187.7	3.0753	50
SN201248	12	184.9	3.0695	50
SN201248	13	186.7	3.0649	50
SN201248	14	187.2	3.0684	50
SN201248	15	187.2	3.0712	50
SN201248	16	186.7	3.0775	50
SN201248	17	188.1	3.0662	50

SN201248	1	293.7	4.2906	97.5
SN201248	2	294.6	4.2926	97.5
SN201248	3	295.6	4.2952	97.5
SN201248	4	293.7	4.3143	97.5
SN201248	5	296	4.3239	97.5
SN201248	6	298.8	4.3509	97.5
SN201248	7	294.2	4.2752	97.5
SN201248	8	296	4.2932	97.5
SN201248	9	293.7	4.2966	97.5
SN201248	10	296	4.3162	97.5
SN201248	11	296	4.3024	97.5
SN201248	12	296	4.3019	97.5
SN201248	13	293.7	4.2998	97.5
SN201248	14	293.2	4.3094	97.5
SN201248	15	295.1	4.3329	97.5
SN201248	16	295.6	4.3109	97.5
SN201248	17	293.7	4.3171	97.5
SN201249	1	394.1	5.3254	148
SN201249	2	393.1	5.3052	148
SN201249	3	392.6	5.3039	148
SN201249	4	394.6	5.3457	148
SN201249	5	425.2	5.2677	148
SN201249	6	384.6	5.3374	148
SN201249	7	344.6	5.3378	148
SN201249	8	387.6	5.2574	148
SN201249	9	393.6	5.3213	148
SN201249	10	393.6	5.3228	148
SN201249	11	407.2	5.3244	148
SN201249	12	388.1	5.2379	148
SN201249	13	389.6	5.2955	148
SN201249	14	389.1	5.2802	148
SN201249	15	388.6	5.2657	148
SN201249	16	388.6	5.2662	148
SN201249	17	391.1	5.2681	148
SN201249	1	118.2	2.1563	25
SN201249	2	117.2	2.1557	25
SN201249	3	116.2	2.1584	25
SN201249	4	116.2	2.1572	25
SN201249	5	116.2	2.1552	25
SN201249	6	118.2	2.1657	25
SN201249	7	116.7	2.1639	25

SN201249	8	118.2	2.1592	25
SN201249	9	117.2	2.1689	25
SN201249	10	117.2	2.1447	25
SN201249	11	115.7	2.1552	25
SN201249	12	117.2	2.1429	25
SN201249	13	116.7	2.1397	25
SN201249	14	115.2	2.1415	25
SN201249	15	118.2	2.1573	25
SN201249	16	118.7	2.1615	25
SN201249	17	117.2	2.1533	25
SN201249	1	186.8	3.0841	50
SN201249	2	183.3	3.0568	50
SN201249	3	184.3	3.066	50
SN201249	4	184.3	3.0599	50
SN201249	5	183.3	3.05	50
SN201249	6	184.8	3.0627	50
SN201249	7	185.3	3.0895	50
SN201249	8	187.8	3.0733	50
SN201249	9	188.3	3.0753	50
SN201249	10	182.3	3.049	50
SN201249	11	185.3	3.0724	50
SN201249	12	187.3	3.0712	50
SN201249	13	186.8	3.0842	50
SN201249	14	183.3	3.0496	50
SN201249	15	184.3	3.0672	50
SN201249	16	186.3	3.0763	50
SN201249	17	184.3	3.0847	50
SN201249	1	293	4.3301	97.5
SN201249	2	294.5	4.3324	97.5
SN201249	3	290	4.2722	97.5
SN201249	4	292.5	4.312	97.5
SN201249	5	289.5	4.2572	97.5
SN201249	6	292	4.3053	97.5
SN201249	7	291.5	4.2998	97.5
SN201249	8	292	4.3234	97.5
SN201249	9	291.5	4.331	97.5
SN201249	10	290.5	4.3131	97.5
SN201249	11	288.5	4.2962	97.5
SN201249	12	290	4.2946	97.5
SN201249	13	289	4.3009	97.5
SN201249	14	290.5	4.2889	97.5

SN201249	15	292.5	4.3329	97.5
SN201249	16	288.5	4.2672	97.5
SN201249	17	291	4.3227	97.5

Appendix C - System Mass

To ensure that variability in the helmet system was not affecting the results, the tangible variable of mass was compared to peak acceleration. The small variations in pad mass (in the case of Team Wendy) do not appear to correlate to peak acceleration. These data show that helmet system manufacturing tolerances are well within the error of the test. Pad and system masses are shown in Table 3.

Table C-1: Helmet System Mass

	Total Pad Mass (grams)			Total Helmet System Mass (grams)		
Size	**N**	**Mean**	**Std Dev**	**N**	**Mean**	**Std Dev**
Small	252	92.03	0.79	252	1328.15	9.01
Medium	252	94.33	2.54	252	1447.29	20.93
Large	252	91.22	1.29	252	1475.50	22.48
X-large	252	91.48	3.84	252	1638.88	56.08
All	1008	92.27	2.71	1008	1472.45	115.51

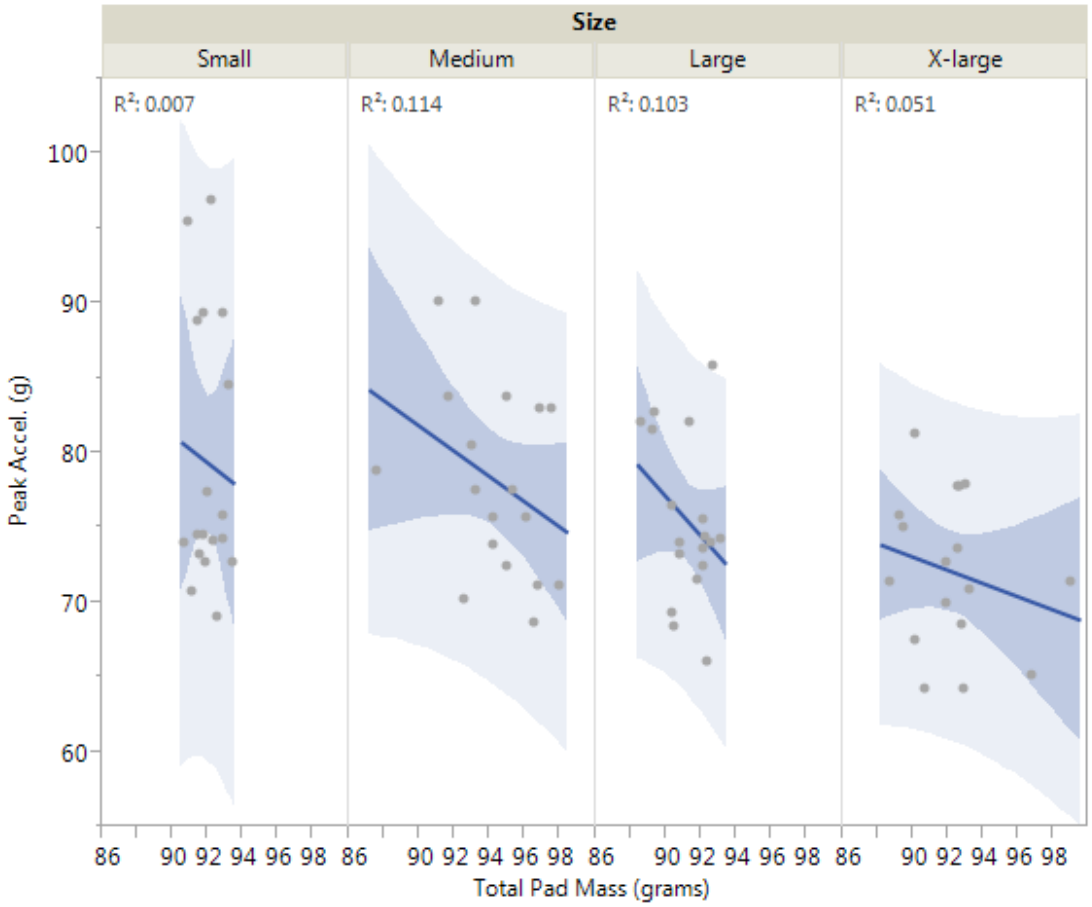

Figure C-1: Helmet pad mass correlated to peak acceleration

This page intentionally left blank

Appendix D - Historical Data comparison

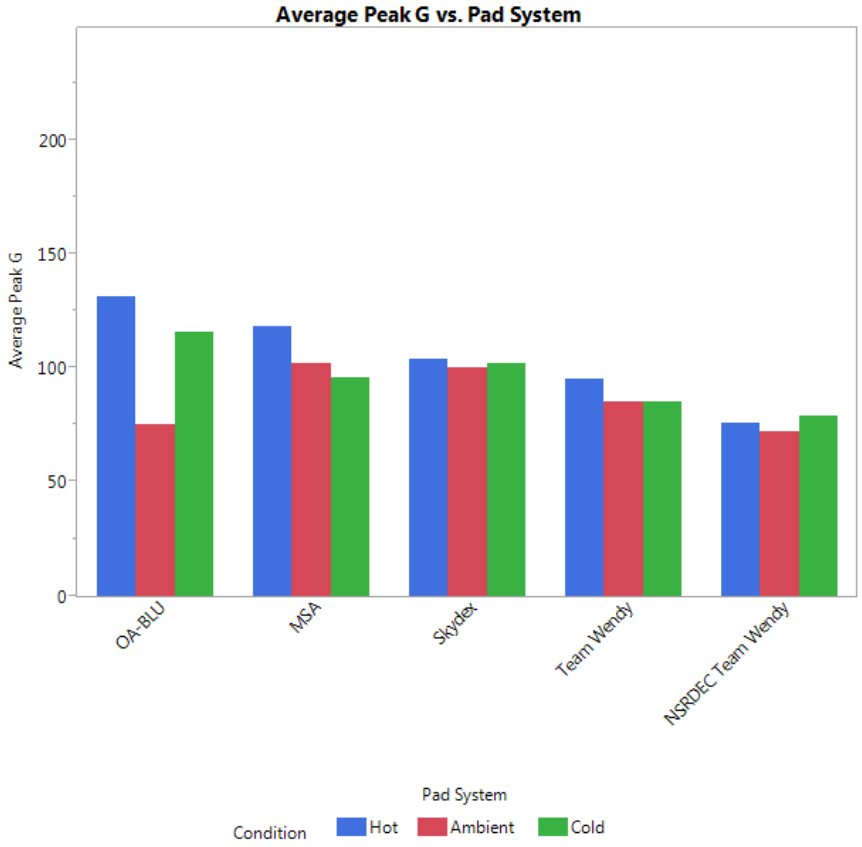

Figure D-1: Average peak acceleration of various pad systems at 10 ft/s

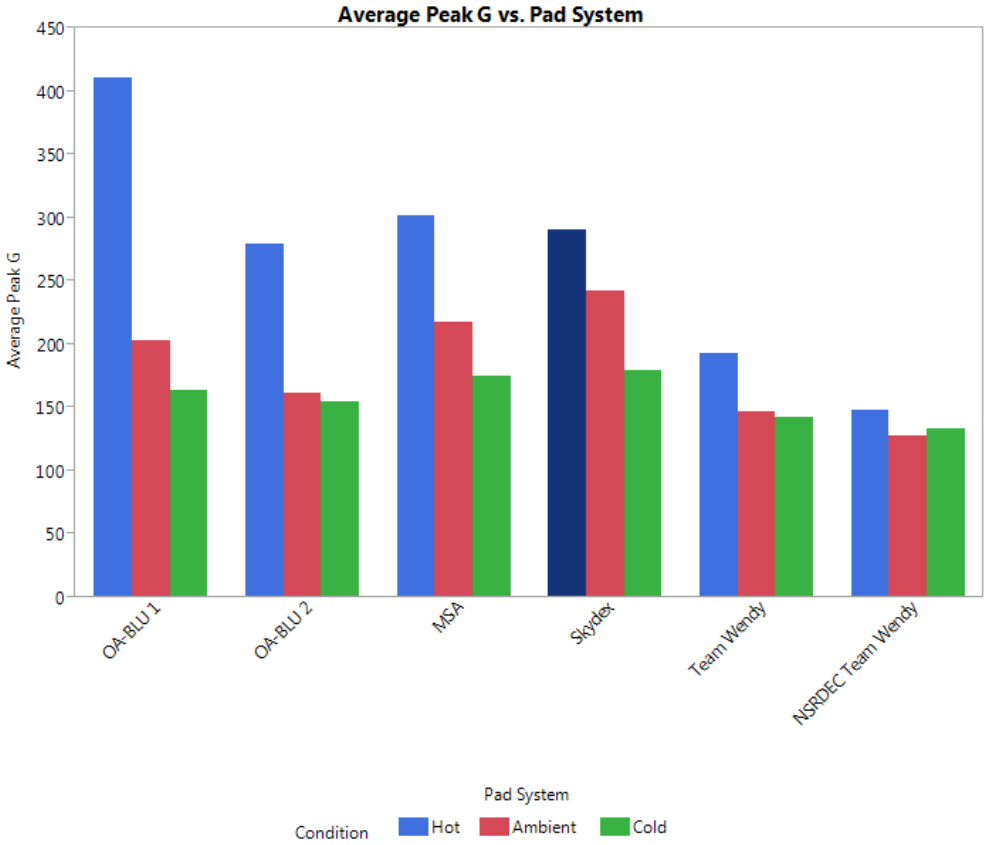

Figure D-2: Average peak acceleration of various pad systems at 14.1 ft/s

Table D-1: Aggregate Data (all conditions)

	Velocity = 10ft/s					Velocity = 14.1ft/s					
	OA-BLU	MSA	Skydex	Team Wendy	NSRDEC Team Wendy	OA-BLU 1	OA-BLU 2	MSA	Skydex	Team Wendy	NSRDEC Team Wendy
Average Peak Acc. (g)	107	106	102	89	74.97	259	198	232	238	161	136.65
Standard Deviation	43	27	14	16	16.97	160	98	116	103	58	36.43
Max Peak Acc. (g)	278	211	141	162	115.3	546	496	501	495	422	239.5
N	125	109	126	116	128	126	126	126	126	126	84